COMPARISON OF SURF ZONE TURBULENCE AND FLOW STRUCTURES IN SPILLING AND PLUNGING WAVES

Kessie Govender, Cape Peninsula University of Technology, South Africa, govenderk@cput.ac.za
Gary Mocke, CoMarEng Advisory, gpmocke@gmail.com

INTRODUCTION

Wave breaker generated turbulence and flow fields are a major contributor to sediment suspension and transport, hence a quantitative understanding is critical for predicting coastal erosion. Laboratory and field studies have been carried out in both spilling and plunging waves case to measure these fields, primarily using LDA to measure wave breaker turbulence in non-aerated areas of wave flumes. Although more recent measurement campaigns have included imaging techniques most of the recordings have been confined to below the wave trough due to the presence of wave bubbles higher in the water column. This situation is aggravated in plunging waves, with high levels of aeration through the full water column, especially near the break point. Over the past two decades the authors (Govender et al. (2002a,2002b,2023)) have developed a combination of particle and bubble imaging techniques that allows us to measure fluid velocities through the entire water column, including the wave roller in both spilling and plunging waves. In this paper we undertake a comparison of the flow structures and turbulence between spilling and plunging waves in the surf zone. We present comparative plots of the experimental measurements of mean and turbulent velocities, turbulence kinetic energy, and turbulence shear stress. The paper also discusses the evolution of turbulent intensities at various surf zone locations and levels through the water column over the wave period, which is an important consideration for mathematical modeling of sediment dynamics.

EXPERIMENTAL SETUP AND CONDITIONS

The experiments were conducted in a glass walled flume, featuring visualization equipment. Waves broke on 1:20 slope beach. The schematic of the bottom profile and measurement positions are shown in figure 1 below. Plunging waves having period of 2.5 s and a deep-water wave height of 12 cm and spilling wave having period of 1.11 s and a wave height of 16 cm were used. In the spilling wave the velocities were measured at three positions in the surf zone (labeled S1, S2 and S3 in figure 1) whilst in the plunging wave measurements were conducted at six positions (labeled P1 to P6).

Measurement of the fluid velocities over the entire water column and through the outer and inner surf zones were obtained using video cameras and image analysis techniques utilizing particle and bubble image velocimetry. The measurement setup that was used in the experiments to measure fluid velocities is shown in figure 2 (Govender (2002a)). The setup has been designed to produce two images of the seeded and aerated flow spaced in time by a predetermined time interval. The instantaneous flow fields were extracted from these images using cross correlation techniques.

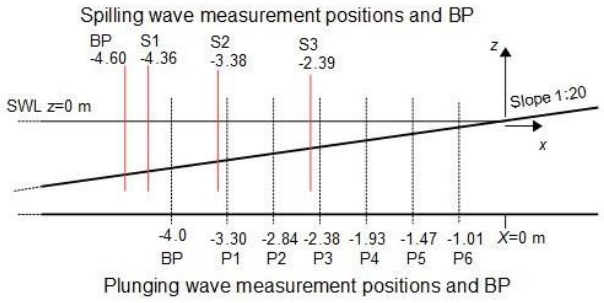

Figure 1 - Schematic of the wave flume and measurement positions.

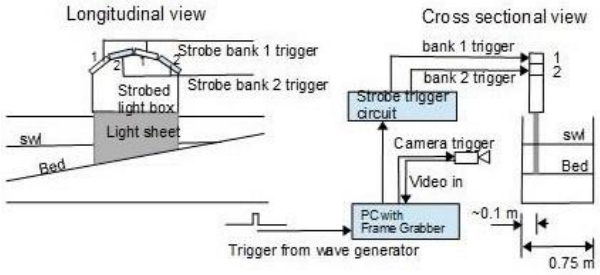

Figure 2 - Schematic of the measurement setup.

RESULTS

The instantaneous velocity flow fields are analyzed to extract key features such as mean velocities, turbulence intensities, turbulent kinetic energy (TKE), Reynolds and wave shear stresses. Shown below are spilling and plunging wave case comparisons of nondimensionalized values for undertow, TKE and Reynold shear stress corresponding to two comparable positions (h/hb~0.7 and h/hb~0.5) along the wave flume.

Figure 3 shows the plot of the time averaged horizontal velocity as a function of depth. Near the break point at P2 and S2, the undertow in both cases is not fully developed and is still transitioning from pre-breaking to fully developed. While the forward velocity profiles are similar, the values are higher in the plunging case. Further in the surf zone at P4 and S3, the profiles of forward velocities and undertow are similar. Note that the difference in vertical extent of the forward profiles at P4 and S3 is due

to the different wave heights relative to the water depth at these positions.

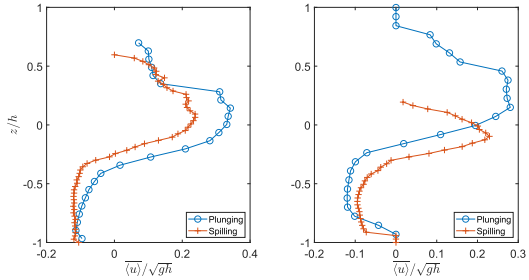

Figure 3 - Plot of the undertow (left plot) in the plunging wave at P2 (h/h_b=0.75) and spilling wave at S2 (h/h_b =0.72) and (right plot) in the plunging wave at P4 (h/hb=0.54) and spilling wave at S3 (h/h_b =0.57).

The plot of the time averaged TKE is shown in figure 4. These plots show distinct differences between the plunging and spilling waves. The TKE is almost uniform with a small linear increase above the bed for the spilling case whereas it mainly increases exponentially in the plunging wave case, The values of TKE are much higher in the plunging wave, with considerable turbulent intensities above the approximated trough level. This is due to the higher concentration of vortices in the plunging wave. Although there is evidence of convection, especially in the plunging wave case near the break point, the exponential signatures suggest significant diffusion from the near surface area. Observations of TKE levels over the wave period also show maintenance of sufficiently elevated levels suggesting that a time averaged turbulence model could be representative. Figure 5 shows the plot of the time averaged turbulence Reynolds stress. These plots also show distinct differences between the plunging and spilling waves. Higher levels of Reynolds shear stress occur in the plunging wave throughout the water column. Most of the shear stress is confined between the bed and still water level. On the average, there is a linear increase of shear stress from the bed upwards in the spilling case, while there is a more exponential increase in the plunging case. The contribution of the bottom boundary layer is clearly noticeable in the spilling wave at S2 and S3.

These measurements have important implications for the modeling of sediment suspension and transport in the surf zone, notably in terms of quantifying the vertical structure of suspended sediment concentrations. The results also support the approach earlier adopted by Mocke (2001) and other authors in representing sediment dynamics in the surf zone by time averaged eddy viscosity modeling.

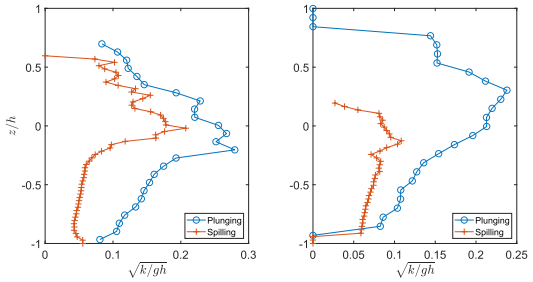

Figure 4 - Plot of the time averaged TKE (left plot) in the plunging wave at P2 (h/h_b =0.75) and spilling wave at S2 (h/h_b =0.72) and (right plot) in the plunging wave at P4 (h/h_b =0.54) and spilling wave at S3 (h/h_b =0.57).

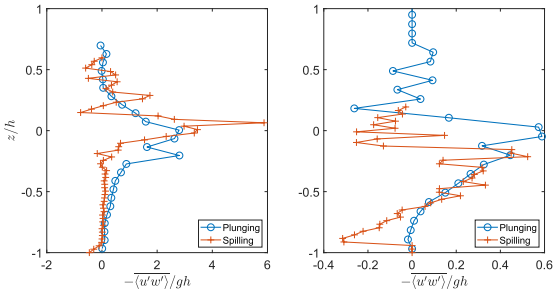

Figure 5 - Plot of the time averaged turbulence Reynolds stress (left plot) in the plunging wave at P2 ($x10^{-2}$) (h/h_b =0.75) and spilling wave at S2 (x 10^{-3}) (h/hb=0.72) and (right plot) in the plunging wave at P4 ($x10^{-2}$) (h/h_b =0.54) and spilling wave at S3 ($x10^{-3}$) (h/h_b =0.57). Note the different multiplication scale factors.

The presentation will include details of both time dependent and phase averaged features of velocities, and turbulence kinetic energy (TKE) over the wave cycle, also further discussing implications for surf zone sediment dynamics modeling.

REFERENCES

Govender, Alport, Mocke, Michallet (2002a): Video measurements of fluid velocities and water levels in breaking waves, Phyisca Scripta, T 97, pp.152-159.

Govender, Mocke and Alport (2002b): Video-imaged surf zone wave and roller structures
and flow fields, JGR, vol. 107, pp. 3702:1-21.

Govender, Mukaro, Mocke (2023): Laboratory measurements of mean and turbulence velocities and shear stresses through the wave roller in strong plunging waves, Coastal Engineering, vol. 180, pp. 104254.

Mocke, G. P. (2001): Structure and modeling of surf zone turbulence due to wave breaking. J. Geophys. Res., 106, 17 039–17 057